EFFECTS OF HALLCURRENTS WITH HEAT AND MASS TRANSFER ON THE PERISTALTIC TRANSPORT OF A CASSON FLUID THROUGH A POROUS MEDIUM IN A VERTICAL CIRCULAR CYLINDER

Nabil T. M. EL-DABE, Galal M. MOATIMID, Mona A. A. MOHAMED, Yasmeen M. MOHAMED*

Department of Math., Faculty of Education, Ain Shams University, Roxy, Cairo, Egypt
* Corresponding author E-mail: yasmeenmostafa303@yahoo.com

In the current paper, the peristaltic transport of a non - Newtonian fluid obeying a Casson model with heat and mass transfer inside a vertical circular cylinder is studied. The considered system is affected by a strong horizontal uniform magnetic field together with the heat radiation and the Hall current. The problem is modulated mathematically by a system of partial differential equations that describe the basic behavior of the fluid motion. The boundary value problem is analytically solved with the appropriate boundary conditions in accordance with the special case, in the absence of the Eckert number E_c. The solutions are obtained in terms of the modified Bessel function of the first kind. Again, in the general case, the system is solved by means of the Homotopy perturbation and then numerically through the Runge – Kutta Merson with a shooting technique. A comparison is done between these two methods. Therefore, the velocity, temperature and concentration distributions are obtained. A set of diagrams are plotted to illustrate the influence of the various physical parameters in the forgoing distributions. Finally, the trapping phenomenon is also discussed.

Keywords: *Peristaltic flow, Casson model, Hall Current, Porous medium, Heat and mass transfer.*

1. Introduction

The mechanism of peristalsis, in both mechanical and physiological situations, has become of great importance in many scientific researches. Several theoretical and experimental attempts have been made to understand peristaltic influence in different situations. The scientists have exerted their efforts concerning the peristaltic flow of liquids. The problem of peristalsis with heat and mass transfer is analyzed by Hina et al. [1],chemical reaction is taken into account. Their study not only based on long wavelength and low Reynolds number approximation but also on a small Grashof number. Peristaltic flow of viscous fluid in an asymmetric inclined channel with heat transfer and the influence of an inclined magnetic field are studied by Noreen et al. [2]. In their work, long wavelength and low Reynolds number approximation is utilized. Peristaltic motion of a non-Newtonian nano fluid with heat transfer through a porous medium inside a vertical tube is investigated by El-dabe et al. [3]. Rung-Kutta Merson method and a Newtonian iteration in a shooting and matching technique are also

utilized. The influence of heat and mass transfer on the peristaltic flow of magneto hydrodynamic Eyring- Powell fluid is discussed by Shaaban et al. [4]. Finite-difference technique is used for solving their governing system of equations. The impact of compliant walls on peristaltically induced flow of Sutterby fluid in a vertical channel is studied by Hayat et al. [5]. The problem formulation is based on neglecting the inertial effects and using long wavelength approximation. In their work, they observed that the velocity and temperature distributions are greater than of viscous fluid. The effects of partial slip on the peristaltic flow of a MHD Newtonian fluid are analyzed by Nadeem et al. [6]. The solutions of the governing system of equations are obtained by means of Adomian decomposition method. They observed that the temperature distribution decreased with the increasing of slip parameter and magnetic field parameter. Meanwhile, it increased with the increasing of the Eckert number.

The Hall effect is an ideal magnetic field sensing technology, the influence of the Hall current on a rotating unsteady flow of a conducting second grade fluid on an infinite oscillating plate is analyzed by Hayat et al. [7]., also, the Laplace transform and the regular perturbation method are utilized to obtain the solutions of the governing equations. They observed that the boundary layer thickness had increased with the increasing of the Hall parameter at fixed magnetic field parameter. Peristaltic transport obeying Walter's B fluid in an asymmetric channel is discussed by Mehmood et al. [8]. Their problem is affected by heat and mass transfer, regular perturbation method is utilized for solving their governing system of equations of motion. The peristaltic flow of an incompressible, electrically conducting Williamson fluid is investigated by Eldabe et al. [9]. Hall effects, viscous dissipation and Joule heating are taken into account. Peristaltic motion induced by sinusoidal traveling wave of incompressible, electrically conducting Maxwell fluid is discussed by El Koumy et al. [10], Hall current with constant magnetic field is taken into account and perturbation expansion in terms of small amplitude ratio is utilized to obtain their solutions.

Casson fluids are found to be applicable in developing models for blood oxygenator. Magneto hydrodynamic (MHD) flow and heat transfer of electrically conducting viscoelastic fluids is analyzed by Akbar et al. [11]. Casson model is utilized to describe the viscoelastic behavior. They found that the temperature is increased with the increasing of the Casson parameter, Hartmann number, velocity slip, eccentricity parameter, thermal slip and also Brinkmann (dissipation) number. In addition, they found that the increasing in Casson parameter led to increase in the size of the trapped bolus. Casson fluid flow over a vertical porous surface with chemical reaction in the presence of magnetic field is investigated by Arthur et al. [12]. Their system of partial differential equations, which describe the problem, is solved numerically by means of the Newton Raphson shooting method with the aid of the Fourth-order Runge-Kutta algorithm. Viscous incompressible electrically conducting micropolar flow is investigated by Ali et al. [13]. Thermal radiation and viscous dissipation are taken into account. Quasi linearization technique is utilized to solve their coupled system of ordinary differential equations. The impact of pressure stress work and thermal radiation on free convection flow around a sphere is studied by Elbashbeshyet al. [14]. Porous medium with Newtonian heating are taken into consideration. Finite difference technique is utilized to solve their system of nonlinear partial differential equations. Radially varying magnetic field effect on peristaltic motion obeying Jeffery model between two co-axial tubes is analyzed by Eldabe and Abou-zeid [15]. Heat and mass transfer are taken into consideration. Their system of equations is solved analytically using regular perturbation technique.

The aim of this paper is to extend the work of Vasudev et al. [16] but in case of the non-Newtonian fluid which obeying Casson model [12]. The present work includes, also, the concentration equation. Hall current with heat and mass transfer are taken into account as well as viscous dissipation, chemical reaction and radiation absorption. The boundary value problem is analytically solved with the appropriate boundary conditions in accordance with the special case, in the absence of the Eckert number E_c; the solutions are obtained in terms of the modified Bessel function of the first kind. Again, in the general case, the system is solved analytically by means of the homotopy perturbation method and numerically using Runge – Kutta Merson with the shooting technique. A comparison is done between these two methods. Therefore, the velocity, temperature and concentration distributions are obtained. A set of diagrams are plotted to illustrate the influence of the various physical parameters in the forgoing distributions. Finally, the trapping phenomenon is discussed and illustrated.

2. Mathematical formulation of the problem

Consider the peristaltic flow of an incompressible non-Newtonian fluid through a vertical tube. The axisymmetric cylindrical polar coordinate system *(R, Z)* are used, where *R*-coordinate is along the radial coordinate of the tube and *Z*-coordinate coincides with axis of the tube see Fig. 1.

The geometry of the tube wall is defined as:

$$R = H(Z,t) = a + b\sin(\frac{(2\pi(Z-ct))}{\lambda}), \tag{1}$$

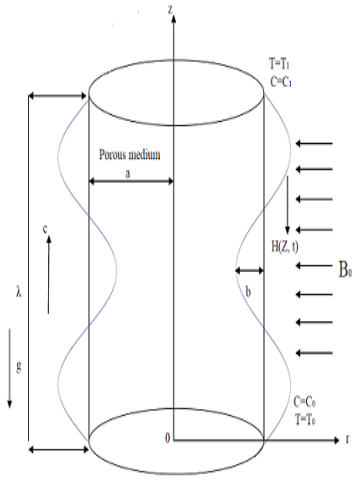

Figure 1. Physical model and coordinates system

For the unsteady two-dimensional flow, the velocity components, temperature and concentration may be written as follows:

$$V = \big(U(R,Z), 0, W(R,Z)\big), \quad T = T(R,Z), \quad C = C(R,Z),$$

The appropriate boundary conditions are defined as [16]:

$$\frac{\partial W}{\partial R} = 0, \quad \frac{\partial T}{\partial R} = 0, \quad \frac{\partial C}{\partial R} = 0 \qquad at\ R = 0 \tag{2}$$

$$W = 0, \quad T = T_0, \quad C = C_0 \qquad at\ R = H(3)$$

Introducing the following transformations between the fixed and moving frames as follows:

$$z = Z - ct, \quad r = R, \quad w = W - c, \tag{4}$$

The current density J including the Hall effect may be written [9] as:

$$J = \sigma[\big(\underline{V} \wedge \underline{B}\big) - \frac{1}{en_e}(\underline{J} \wedge \underline{B})] \tag{5}$$

The governing dimensional equations of motion may be listed as follows:

$$\frac{\partial u}{\partial r} + \frac{u}{r} + \frac{\partial w}{\partial z} = 0, \tag{6}$$

$$u\frac{\partial u}{\partial r}+w\frac{\partial u}{\partial z}=-\frac{1}{\rho}\frac{\partial P}{\partial r}+\frac{\mu_B}{\rho}\left(1+\frac{p_y}{\mu_B\sqrt{2\pi c}}\right)\left[\frac{\partial^2 u}{\partial z^2}+2\left(\frac{\partial^2 u}{\partial r^2}+\frac{1}{r}\frac{\partial u}{\partial r}-\frac{u}{r^2}\right)\right]-\frac{\mu_B}{\rho K_0}u-\left[\frac{\sigma {B_0}^2}{\rho\left(1+\frac{\sigma {B_0}^2}{e\,n_e}\right)}\right]\left[u+\left(\frac{\sigma B_0}{e\,n_e}\right)(w+c)\right], \quad (7)$$

$$u\frac{\partial w}{\partial r}+w\frac{\partial w}{\partial z}=-\frac{1}{\rho}\frac{\partial P}{\partial z}+\frac{\mu_B}{\rho}\left(1+\frac{p_y}{\mu_B\sqrt{2\pi c}}\right)\left[2\frac{\partial^2 w}{\partial z^2}+\frac{\partial^2 w}{\partial r^2}+\frac{1}{r}\frac{\partial w}{\partial r}+\frac{\partial^2 u}{\partial r\partial z}+\frac{1}{r}\frac{\partial u}{\partial r}\right]-\frac{\mu_B}{\rho K_0}(w+c)+g\alpha_C(C-C_0)+g\alpha_T(T-T_0)-\left[\frac{\sigma {B_0}^2}{\rho\left(1+\frac{\sigma {B_0}^2}{e\,n_e}\right)}\right]\left[w+\left(\frac{\sigma B_0}{e\,n_e}\right)u\right], \quad (8)$$

$$\rho c_p\left(u\frac{\partial T}{\partial r}+w\frac{\partial T}{\partial z}\right)=K\left[\frac{\partial^2 T}{\partial r^2}+\frac{1}{r}\frac{\partial T}{\partial r}+\frac{\partial^2 T}{\partial z^2}\right]+Q_0+\left(\mu_B+\frac{p_y}{\sqrt{2\pi c}}\right)\left[2\left(\frac{\partial u}{\partial r}\right)^2+2\left(\frac{\partial w}{\partial z}\right)^2+2\left(\frac{\partial u}{\partial r}\right)\left(\frac{\partial w}{\partial z}\right)+\left(\frac{\partial u}{\partial z}\right)^2+\left(\frac{\partial w}{\partial r}\right)^2\right]+\frac{16\sigma^* {T_0}^3}{3k^*}\left[\frac{\partial^2 T}{\partial r^2}+\frac{1}{r}\frac{\partial T}{\partial r}\right], \quad (9)$$

$$u\frac{\partial C}{\partial r}+w\frac{\partial C}{\partial z}=D\left[\frac{\partial^2 C}{\partial r^2}+\frac{1}{r}\frac{\partial C}{\partial r}+\frac{\partial^2 C}{\partial z^2}\right]-K_1(C-C_0)+\frac{DK_T}{T_m}\left[\frac{\partial^2 T}{\partial r^2}+\frac{1}{r}\frac{\partial T}{\partial r}+\frac{\partial^2 T}{\partial z^2}\right]. \quad (10)$$

It is convenient to write the above Eqs. (6)- (10) with the boundary conditions (2) and (3) after a transformation in an appropriate dimensionless form. This can be done in a number of ways depending primarily on the choice of the characteristic length, mass and time. Consider the following dimensionless forms:

The characteristic length = a, the characteristic mass=ρa^3, and the characteristic time= a/c. The other dimensionless quantities are given by:

$$\overline{r}=\frac{r}{a},\overline{z}=\frac{z}{\lambda},\overline{u}=\frac{u}{c},\overline{w}=\frac{w}{c},\emptyset=\frac{b}{a},\overline{P}=\frac{Pa^2}{\mu_B},\Phi=\frac{C-C_0}{C_0},\ \theta=\frac{T-T_0}{T_0},D_a=\frac{K_0}{a^2},\gamma=\frac{\rho\,a^2K_1}{\mu_B},P_r=\frac{\mu_B c_p}{K},R_e=\frac{\rho ac}{\mu_B},S_c=\frac{\mu_B}{\rho D},S_r=\frac{\rho DT_0K_T}{\mu_B T_m C_0},E_c=\frac{\mu_B c^2}{KT_0},G_{rC}=\frac{g\rho a^2\alpha_C C_0}{\mu_B c},G_{rT}=\frac{a^2 g\rho\alpha_T T_0}{\mu_B c},m=\frac{\sigma B_0}{en_e},M^2=\frac{\sigma {B_0}^2a^2}{\mu_B},R_n=\frac{4{T_0}^3\sigma^*}{Kk^*},\delta=\frac{a}{\lambda},\beta=\frac{\mu_B\sqrt{2\pi c}}{p_y},h=\frac{H(z)}{a}=1+\emptyset\sin 2\pi z,\ and\ \beta_1=\frac{Q_0a^2}{KT_0}. \quad (11)$$

The governing equations of motion in dimensionless form after using Eq. (11) and dropping the bar mark may be listed as follows:

$$\frac{\partial u}{\partial r}+\frac{u}{r}+\frac{\partial w}{\partial z}=0, \quad (12)$$

$$R_e\delta^3\left(u\frac{\partial u}{\partial r}+w\frac{\partial u}{\partial z}\right)=-\frac{\partial P}{\partial r}-\frac{\delta^2}{D_a}u+\left(1+\frac{1}{\beta}\right)\left[\delta^4\frac{\partial^2 u}{\partial z^2}+2\delta^2\left(\frac{\partial^2 u}{\partial r^2}+\frac{1}{r}\frac{\partial u}{\partial r}-\frac{u}{r^2}\right)+\delta^2\frac{\partial^2 w}{\partial r\partial z}\right]-M^2\delta^2u-M^2\delta(w+1), \quad (13)$$

$$R_e\delta\left(u\frac{\partial w}{\partial r}+w\frac{\partial w}{\partial z}\right)=-\frac{\partial P}{\partial z}+\left(1+\frac{1}{\beta}\right)\left[2\delta^2\frac{\partial^2 u}{\partial z^2}+\left(\frac{\partial^2 w}{\partial r^2}+\frac{1}{r}\frac{\partial w}{\partial r}\right)+\delta^2\frac{\partial^2 u}{\partial r\partial z}+\frac{\delta^2}{r}\frac{\partial u}{\partial z}\right]-N^2(w+1)-\left(\frac{mM^2\delta}{1+m^2}\right)u+G_{rC}\Phi+G_{rT}\theta, \quad (14)$$

$$R_e\,\delta\,P_r\left(u\frac{\partial\theta}{\partial r}+w\frac{\partial\theta}{\partial z}\right)=\left(1+\frac{4}{3}R_n\right)\left(\frac{\partial^2\theta}{\partial r^2}+\frac{1}{r}\frac{\partial\theta}{\partial r}\right)+\delta^2\frac{\partial^2\theta}{\partial z^2}+\beta_1+E_c\left(1+\frac{1}{\beta}\right)[2\delta^2\left(\frac{\partial u}{\partial r}\right)^2+2\delta^2\left(\frac{\partial w}{\partial z}\right)^2+2\delta\left(\frac{\partial u}{\partial z}\right)\left(\frac{\partial w}{\partial r}\right)+\delta^4\left(\frac{\partial u}{\partial z}\right)^2+\left(\frac{\partial w}{\partial r}\right)^2+2\delta^2\left(\frac{u^2}{r^2}\right)] \quad (15)$$

and

$$R_e\,\delta\,S_c\left(u\frac{\partial\Phi}{\partial r}+w\frac{\partial\Phi}{\partial z}\right)=\frac{\partial^2\Phi}{\partial r^2}+\frac{1}{r}\frac{\partial\Phi}{\partial r}+\delta^2\frac{\partial^2\Phi}{\partial z^2}+S_cS_r\left[\frac{\partial^2\theta}{\partial r^2}+\frac{1}{r}\frac{\partial\theta}{\partial r}+\delta^2\frac{\partial^2\theta}{\partial z^2}\right]-\gamma S_c\Phi. \quad (16)$$

Also, the dimensionless appropriate boundary - conditions are given by:

$$\frac{\partial w}{\partial r}=0,\frac{\partial\theta}{\partial r}=0,\frac{\partial\Phi}{\partial r}=0 \qquad at\ r=0 \quad (17)$$

$$w=-1,\theta=0,\Phi=0 \qquad at\ r=h \quad (18)$$

where,
$$N^2=\frac{M^2}{\frac{1}{D_a}+(1+m^2)} \quad (19)$$

The above equations of motion are nonlinear partial differential equations. They cannot be solved in their present form; therefore, an approximation to solve these equations is considered. At this stage, under the assumptions of long wavelength approximation ($\delta \ll 1$) and low Reynolds number ($R_e \rightarrow 0$), these equations may be written as follows:

$$\frac{\partial P}{\partial r} = 0 \tag{20}$$

$$0 = -\frac{\partial P}{\partial z} + \left(1 + \frac{1}{\beta}\right)\left(\frac{1}{r}\frac{\partial}{\partial r}\left(r\frac{\partial w}{\partial r}\right)\right) - N^2(w+1) + G_{rC}\Phi + G_{rT}\theta \tag{21}$$

$$0 = \left(1 + \frac{4}{3}R_n\right)\left[\frac{1}{r}\frac{\partial}{\partial r}\left(r\frac{\partial \theta}{\partial r}\right)\right] + E_c\left(1 + \frac{1}{\beta}\right)\left(\frac{\partial w}{\partial r}\right)^2 + \beta_1, \tag{22}$$

and

$$0 = \left[\frac{1}{r}\frac{\partial}{\partial r}\left(r\frac{\partial \Phi}{\partial r}\right)\right] + S_c S_r\left[\frac{1}{r}\frac{\partial}{\partial r}\left(r\frac{\partial \theta}{\partial r}\right)\right] - \gamma S_c \Phi. \tag{23}$$

It is worthwhile to notice that Eqs. (13) - (16) are more general than these early obtained by Vasudev et al. [16]. In other words, on setting *(*$m = 0,\ G_{rC} = 0,\ R_n = 0,\ S_c = 0,\ S_r = 0,\ E_c = 0,\ \beta \rightarrow \infty$ and $\gamma = 0$),one finds his previous equations (Newtonian case).

3. Method of solution

3.1 Solution in the special case ($\boldsymbol{E_c}$*= 0)*

To relax the mathematical manipulation in solving the resulted Eqs. (20) - (23), the presence of the Eckert number is ignored. In this case, these equations are easily solved to yield the following solutions.

$$\theta = \frac{\beta_1 a_1}{4}(h^2 - r^2), \tag{24}$$

$$\Phi = \left(\frac{S_r a_1 \beta_1}{\gamma}\right)\left[\frac{I_0(n\,r)}{I_0(n\,h)} - 1\right], \tag{25}$$

$$w = \frac{1}{N^2}\frac{dP}{dz}\left[\frac{I_0(L\,r)}{I_0(L\,h)} - 1\right] - 1 + \frac{G_{rT}\beta_1 a_1}{4\,N^2}\left[(h^2 - r^2) + \frac{4}{N^2}\left(1 + \frac{1}{\beta}\right)\left[\frac{I_0(L\,r)}{I_0(L\,h)} - 1\right]\right] + \frac{G_{rC}\beta_1 a_1 S_r}{\gamma\,N^2}\left[\frac{I_0(n\,r)}{I_0(n\,h)} - 1\right]. \tag{26}$$

where, $I_0(..)$ is the modified Bessel function of the first kind and zero order, $L = \sqrt{\frac{N^2\,\beta}{1+\beta}}$ *and* $n = \sqrt{\gamma\,S_c}$.

3.2 Solution in the general case ($\boldsymbol{E_c}$*≠ 0)*

3.2.1Homotopy perturbation solution

In order to consider the general case, in the presence of the Eckert number, a perturbation technique may be useful. Therefore, HPM is utilized. This method is considered as one of the recent perturbation methods. It can be used to solve the ordinary as well as partial differential equations. It combines between the advantages of the Homotopy analysis method (HAM) and the regular perturbation methods. The HPM is first introduced by He [15]. HPM has been successfully applied in a different range of linear as well as nonlinear differential equations by [18 -21]. The method provides us, in a convenient way, an analytical or approximation solution in a wide variety for many problems arising in various fields. Away from the classical and the traditional perturbation methods, the HPM need not a small parameter or a linearization of the zero-order equation. Therefore, through this method, one can put a small parameter $p \in [0, 1]$, p is termed as the embedded Homotopy parameter, as a coefficient in any term of the problem. When $p = 0$, the differential equation takes a simplified

form at which it may has an analytical solution. As p is increased and eventually takes the unity, the equation evolves the two required form. At this step, the expected solution will approach to the desired form.

The HPM is based on the initial approximation, keep in mind that this approximation must satisfy the system of the differential equations as well as the corresponding boundary – conditions. For this purpose, the following relations are defined as:

$$H(p,w) = (1-p)[L(w) - L(w_0)] - p\left(\frac{1}{1+\frac{1}{\beta}}\right)\left[\frac{dP}{dz} + N^2(w+1) - G_{rT}\theta - G_{rC}\Phi\right], \quad (27)$$

$$H(p,\theta) = (1-p)[L(\theta) - L(\theta_0)] + p\left(\frac{1}{1+\frac{4}{3}R_n}\right)\left[\beta_1 + \left(1+\frac{1}{\beta}\right)E_c(\frac{\partial w}{\partial r})^2\right], \quad (28)$$

$$H(p,\Phi) = (1-p)[L(\Phi) - L(\Phi_0)] - p\left(\frac{1}{1+A}\right)\left[\gamma\, S_c\Phi - S_rS_c\left(\frac{\partial^2\theta}{\partial r^2} + \frac{1}{r}\frac{\partial\theta}{\partial r}\right)\right]. \quad (29)$$

with$L(*) = \frac{\partial^2(*)}{\partial r^2} + \frac{1}{r}\frac{\partial(*)}{\partial r}$is the linear operator. The initial approximation may be written as:

$$w_0 = -\frac{r^2}{h^2}, \qquad \theta_0 = r^2 - h^2 \quad and \quad \Phi_0 = r^2 - h^2\ . \quad (30)$$

Any of the distribution functions *w*, $\theta$and Φ may be written as:

$$f(r,p) = \sum_{i=0}^{n} p^i f_i. \quad (31)$$

On using the above power series on the Eqs. (27) - (29) and equating the coefficients of like powers of p on each of them and solving the resulted equations, one obtains the solutions of the different stages of $p^n$the procedure is lengthy but straightforward. The complete solution is obtained by setting $p = 1$. The power series up to the second - order for each of the forgoing distributions may be written as follows:

$$w(r) = -\frac{r^2}{h^2} + (M_1 + M_3)(r^2 - h^2) - (M_2 + M_4)(r^4 - h^4) - M_5(r^6 - h^6), \quad (32)$$

$$\theta(r) = \big((M_6\beta_1) - 1\big)(h^2 - r^2) + (M_6M_7 - M_8)(h^4 - r^4) + M_9(h^6 - r^6), \quad (33)$$

$$\Phi(r) = \frac{1}{36}\left(\frac{\gamma^2 S_C{}^2}{16}\right)(r^6 - h^6) + (1 - M_{11} + \left(\left(\frac{-\gamma\, S_c h^2}{4}\right) + S_rS_c\right)(r^2 - h^2) + \left(\frac{\gamma\, S_c}{16} + M_{10}\left(\frac{\gamma^2 S_C{}^2}{16}\right)\right)(r^4 - h^4). \quad (34)$$

The constants a_1, M_1-M_{11} are defined but excluded here to save space.

3.2.2 Numerical solution

From the forgoing analysis; first, the influence of the Eckert number is ignored and, secondly, when this influence is considered we use the HPT. Now, the whole problem may be solved in accordance with a numerical method. On using the Runge - Kutta Merson with shooting technique, assume the following steps:

Consider the following transformations:

$$w = Y_1, \qquad \theta = Y_3 \quad and \quad \Phi = Y_5. \quad (35)$$

Therefore, Eqs. (20) - (23) may be written as:

$$Y_1' = Y_2\,, Y_2' + \frac{1}{r}Y_2 = \left(\frac{1}{1+\frac{1}{\beta}}\right)\left[\frac{dP}{dz} + N^2(Y_1+1) - G_{rT}Y_3 - G_{rC}Y_5\right], \quad (36)$$

$$Y_3' = Y_4, Y_4' + \frac{1}{r}Y_4 = -a_1\left(\beta_1 + \left(1+\frac{1}{\beta}\right)E_c(Y_2)^2\right), \quad (37)$$

$$Y_5' = Y_6\,, Y_6' + \frac{1}{r}Y_6 = \gamma\, S_cY_5 - S_rS_c\left[Y_4' + \frac{1}{r}Y_4\right]. \quad (38)$$

where, the prime denotes to differentiation with respect to r.

The related boundary conditions in accordance with Eqs. (36) - (38), may be written as:

$$Y_1' = 0,\ Y_3' = 0 \quad and \quad Y_5' = 0 \quad at \quad r = 0, \tag{39}$$

$$Y_1 = -1,\ Y_3 = 0 \quad and \quad Y_5 = 0 \quad at \quad r = h\ . \tag{40}$$

To compute the physical quantities w, θ andΦ, Mathematica package version 9 is used to solve the governing system of Eqs. (36) - (38)along the appropriate boundary conditions (39) and (40). Therefore, modified Newton-Raphson iteration method continues until convergence is achieved [3] and [22].

Now, Nusselt number may be defined as:

$$Nu = \left(\frac{\partial\theta}{\partial r}\right)_{r=h}. \tag{41}$$

4. Numerical discussions

In order to illustrate the quantitative effects of the different physical parameters of the problem on the distributions of the axial velocity w, temperature $\theta$and concentrationΦ, the mathematica software (package 9) is utilized. The effects of the physical parameters such as, Hall parameter m, modified Grashof number G_{rC}, the radiation parameter R_n, Eckert number E_c, pressure gradient dP/dz, Darcy number $D_a$and the non-dimensional heat source/sink parameter $\beta_1$on these distributions are discussed numerically, graphically and illustrated through some Figs.2-4.

The variation of axial velocity w versus the radial coordinate r for different values of R_n, modified Grashof number G_{rC}, m, D_a, E_c, $\beta_1$and dP/dz is illustrated. To make a good comparison between the HPT and the Runge-Kutta numerical technique, the following figures are characterized by the two symbols$H$ and N to indicate the HPM and numerical calculations, respectively. The effect of the Hall parameter m on the axial velocity w is illustrated in Fig. 2. It is observed that the velocity w decreases with the increasing of m. This is in a good agreement with the results that first obtained by Hayat et al. [7]. The influence of is studied; we observed that the axial velocity w increases with the increasing of E_c. Physically, this result are realistic, because of the magnetic field is considered as a retardant force of motion. Also, the increasing of $E_c$makes an increasing of the fluid temperature; this alternately increases the fluid flow. To keep spaces we exclude this figure. At the same time, the numerical calculation shows that the non – dimensional Parameter $\beta_1$behaves like E_c. On the other hand, the other parameters of the problem behave like m. To avoid the repetition, we exclude these figures.

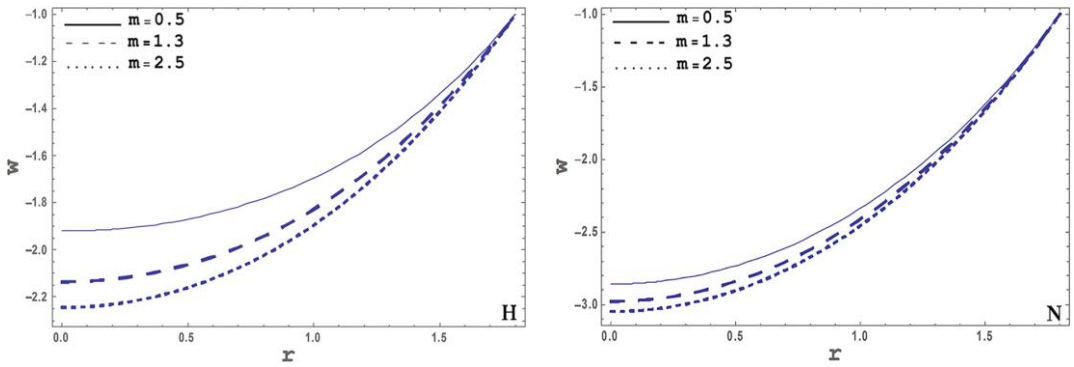

Figure 2. The axial velocity w plotted versus r under the effect of m for M = 1, D_a =0.9, G_{rT} = 0.1, E_c = 3.0, G_{rC} = 0.1, R_n = 0.1, dP/dz = 10, β = 0.5, β_1 = 1, S_c = 0.5, S_r = 1.0, γ = 1.5, z = 0.25, ∅ = 0.8

The variation of temperature distribution θ versus the radial coordinate r for various values of the Eckert number E_c, R_n , $\beta_1$and dP/dz is illustrated. The effect of E_c on the temperature θ is graphed in Fig. 3. As seen from this figure, the temperature distribution is increased with the increasing of E_c.The influence of $R_n$is also studied; we found that the temperature distribution is decreased with the increasing of R_n.. To keep spaces we exclude this figure. This observation gives a good agreement with this obtained by Eldabe et al. [3]. As before, the numerical calculations show that the influence of the physical parameters $\beta_1$anddP/dz, on the temperature distribution θ behave like the Eckert number E_c.

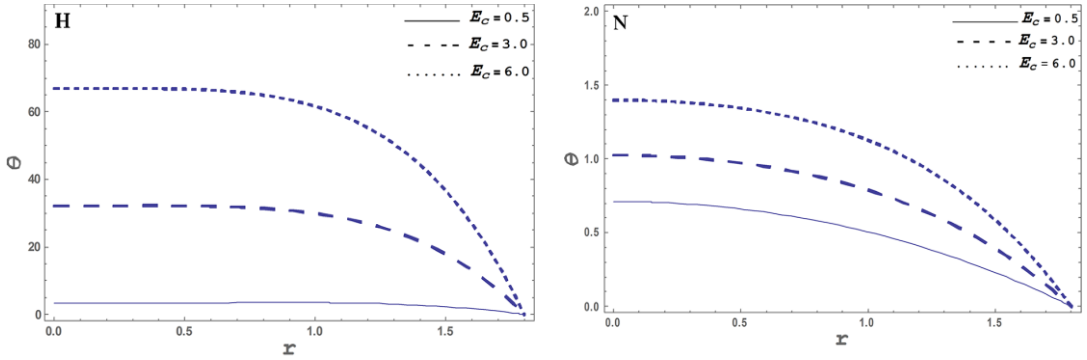

Figure 3. The temperature distribution θ plotted versus r under the effect of E_c for M = 1, D_a = 0.9, G_{rT} = 0.1, m = 0.5, G_{rC} = 0.1, R_n = 0.1, dP/dz = 10, β = 0.5, β_1 = 1, S_c = 0.5, S_r = 1.0, γ = 1.5, z = 0.25, ∅ = 0.8.

The variation of concentration distribution Φ versus the radial coordinate r for several values of E_c , R_n, β_1, $S_c$and S_r is graphed. The effect of the Schmidt number $S_c$on the concentration distribution Φ is depicted through Figs. 4. As seen from this figure, the concentration distribution Φ is decreased with the increasing of S_c. Also, the effect of R_n on the concentration distribution Φ is studied; we observed that the concentration distribution Φ is increased with the increasing of Rn. To keep spaces we exclude this figure. This observation is in a good agreement with this obtained by Hayat et al. [23].

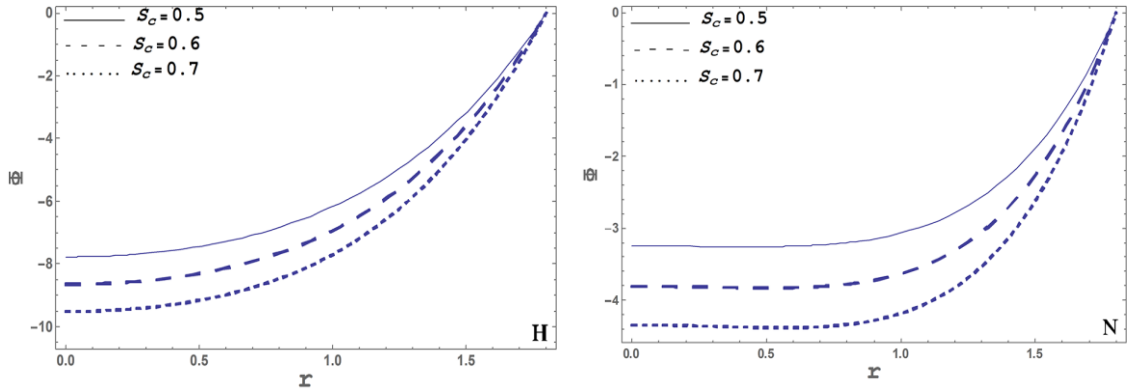

Figure 4. The concentration distribution Φ plotted versus r under the effect of S_c for M = 1, D_a = 0.9, G_{rT} = 0.1, m = 0.5, G_{rC} = 0.1, R_n = 0.1,dP/dz = 10, β = 0.5, β_1 = 1, E_c = 3.0, S_r = 1.0, γ = 1.5, z = 0.25, ∅ = 0.8

5. Trapping

As usual in the hydrodynamic theory, for incompressible fluids in two - dimension, a stream function $\psi(r,z)$ is considered, which is defined as:

$$u = \frac{1}{r}\left(\frac{\partial \psi}{\partial z}\right) \ and \quad w = -\frac{1}{r}\left(\frac{\partial \psi}{\partial r}\right) \ .$$

Now, the stream function$\psi(r,z)$ on the following two cases is defined as:

(1) In the case of the absence of the Eckert number:

$$\psi(r,z) = -\Big[a_2 r\big(2I_1(L\,r) - r\,L\,I_0(L\,h)\big) - \frac{1}{2}r^2 + a_3 r^2(2h^2 - r^2) + a_4 r\big(2I_1(n\,r) - r\,n\,I_0(n\,h)\big)\Big], \tag{42}$$

(2) In the case of the presence of the Eckert number:

$$\psi(r,z) = \frac{r^2}{4\,h^2} + (M_1 + M_3)\left[\frac{h^2 r^2}{2} - \frac{r^4}{4}\right] - (M_2 + M_4)\left[\frac{h^4 r^2}{2} - \frac{r^6}{6}\right] - M_5\left(\frac{h^6 r^2}{2} - \frac{r^8}{8}\right), \tag{43}$$

where $I_1(..)$ is the modified Bessel function of the first kind and first order.

The constants a_2, $a_3$and a_4 are defined in the appendix but excluded here to save space.

In what follows, numerical calculations with the phenomenon of trapping are made. Trapping is an important physical phenomenon in peristaltic motion. It contains a bolus of fluid with a closed streamlines. Generally, the shape of streamlines is as same as the boundary wall in the wave frame. However, under sufficient conditions, some of the streamlines split and enclose a bolus, which moves as a whole with the wave. This phenomenon is defined as trapping [24]. Figures 5illustrated the effect of the thermal Grashof number G_{rT} on the streamlines. It is seen from Fig. 5a. that the size of the trapped bolus is increased with the increasing of G_{rT} in case of the absence of E_c. Also, the bolus size is increased with the increasing of G_{rT} in case of the presence of E_c which is illustrated from Fig. 5b. These results are in agreement with the results those obtained by Noreen [25]. The influence of $D_a$on the streamlines is studied; the bolus size is found to increase with the increasing of the $D_a$in case of the absence of E_c. Meanwhile, in case of the presence of E_c, the bolus size is found to decrease with the increasing of D_a. These results are in agreement with the results those obtained by Akbar et al. [26]. To keep spaces we exclude this figure. Also, the influence of the amplitude ratio $\emptyset$ is studied. It is observed that the bolus size is decreased with the increasing of $\emptyset$ in the case of absence of E_c. Meanwhile, in the case of presence of $E_c$the bolus size is increased with the increasing of $\emptyset$ and the bolus is disappeared at $\emptyset = 0$ in both cases. To avoid the repetition, we exclude these figures.

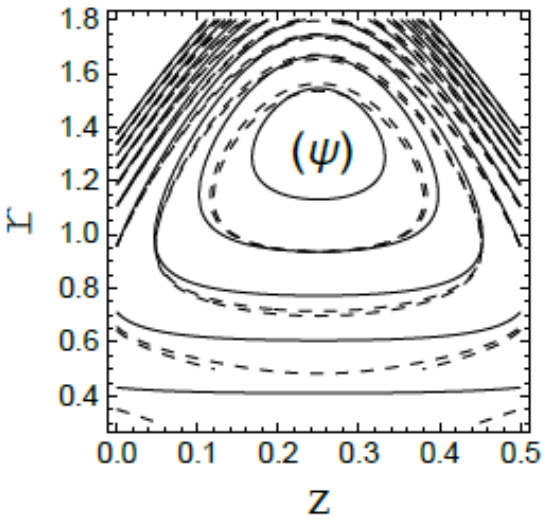

Figure 5a

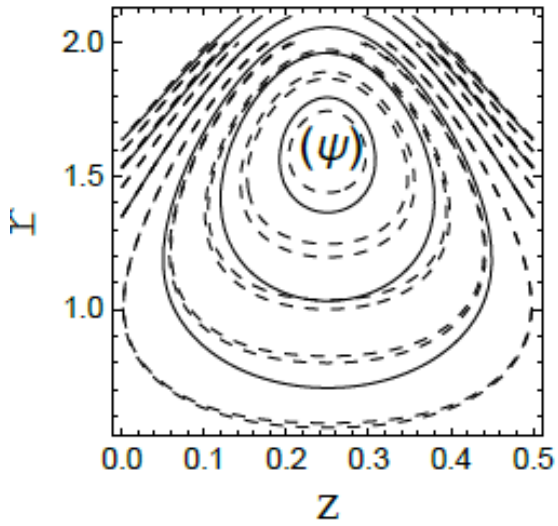

Figure 5b

Figure 5. Streamlines for M = 1, D_a = 0.9, E_c = 3.0, G_{rC} = 0.1, R_n = 0.1, β = 0.5, β_1 = 1, S_c = 0.5, S_r = 1.0, γ = 1.5, z = 0.25, ∅ = 0.6 and for different values of G_{rT} : (a) G_{rT}= 0.1; (b) G_{rT} = 1.5; (c) G_{rT}= 1.8 . Figure 5a at E_c= 0 and Figure 5b at $E_c \neq 0$

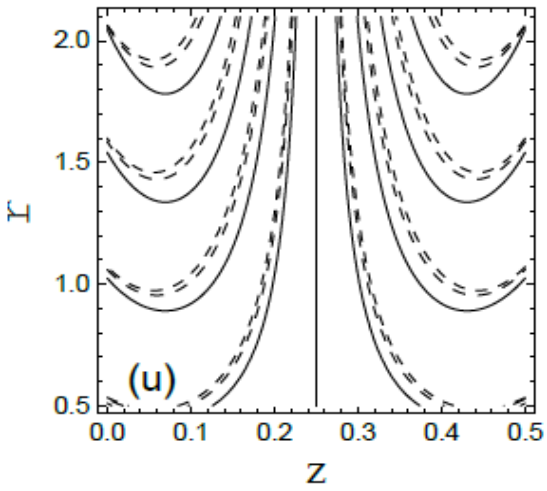

Figure 6a

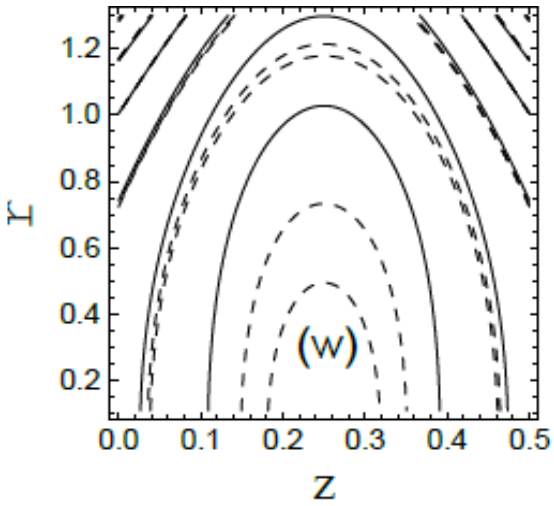

Figure 6b

Figure 6. Contour plot for the radial and axial velocities for M = 1, D_a = 0.9, E_c = 3.0, G_{rC} = 0.1, R_n = 0.1, β = 0.5, β_1 = 1, S_c = 0.5, S_r = 1.0, γ = 1.5, z = 0.25, ∅ = 0.6 and for different values of G_{rT} : (a) G_{rT}= 0.5; (b) G_{rT} = 1.5; (c) G_{rT}= 1.8.

Figure 6 indicates the influence of the thermal Grashof number G_{rT} on the contour plot for the radial and axial velocities $u(r,z)$ and $w(r,z)$ respectively, where the radial direction r is plotted versus the axial one z. It's observed from Fig. 6a that the size of the trapped bolus is decreasing with the increase of G_{rT}. Also, the velocity w is increased. Also, it's observed from Fig. 6b the variation of velocity w is increased with increasing of G_{rT}. Meanwhile, the size of the trapped bolus is decreasing with the increasing of G_{rT}.A comparison for the temperature distribution with the work of Vasudev et al. [16] and the present study is illustrated in Fig. 7. We found that the curves are very close at low values of R_n. A comparison of obtained results for the values of Nusselt number without effect of the Hall currents, chemical reaction parameter, Darcy, Grashof and modified Grashof numbers with those of Eldabe [15] is illustrated through Tab.1.

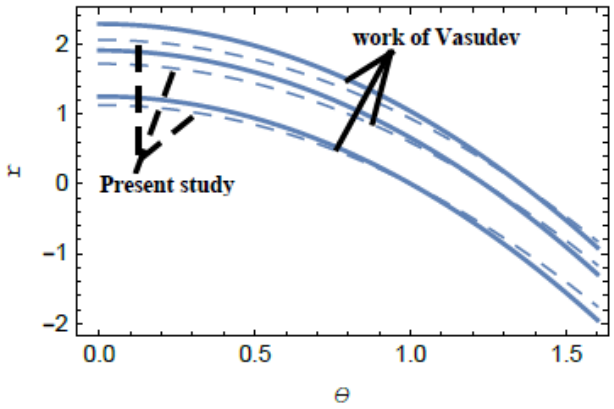

Figure 7. Comparison of temperature distribution with Vasudev work [16].

Table 1. Comparison of Nusselt number Nu between the present results and data obtained by Eldabe and Abou-zeid [15] for various values of S_c with R_n

R_n	S_c	M	E_c	obtained results	Data [15]
2.5	2.5	2	5.5	-0.366222	-0.562607
3.5	3.5	2	5.5	-0.3478	-0.225751
3.5	4.5	2	5.5	-0.3316	-0.225751

6. Conclusion

The purpose of the current study is to investigate the effect of the Hall current on a peristaltic transport of a non - Newtonian flow. The Casson model through a vertical cylinder is taken into account. The system is affected by a strong horizontal uniform magnetic field. In addition, the heat radiation, viscous dissipation, porous media and chemical reaction are considered. The nonlinear governing partial differential equations are presented in a dimensionless form. The resulted system is very complicated to be solved analytically. To relax the mathematical manipulation, the present study depends mainly on the long wavelength approximation in addition with the law Reynolds number. The exact solution is obtained, in the absence of the Eckert number, in terms of the modified Bessel's functions of the first kind. The HPM, in the presence of the Eckert number, is utilized up to the second order. Again, a numerical technique based on the Runge – Kutta Merson with shooting technique is assumed. A set of diagrams are plotted to illustrate the influence of the various physical parameters on the velocity, temperature and concentration distributions. Also, to make a comparison between the analytical solutions and numerical ones. A graphical and data format is compared with some pervious works. A concluding comment may be drawn as follows:

The velocity distribution is increased in accordance with the parameters R_n, β_1 and E_c. Meanwhile, it decreased along the parameters dP/dz , β, $\mathrm{D_a}$, G_{rC} and m. These results are in agreement with the results those obtained by Hayat et al. [7].

The temperature distribution is increased in accordance with the parameters E_c and β_1 . Meanwhile, it decreased along the parameters $\mathrm{R_n}$ and $\mathrm{dP/dz}$. These results are in agreement with the results those obtained by Eldabe et al. [3].

The concentration distribution is increased in accordance with the parameter $\mathrm{R_n}$. Meanwhile, it decreased along the parameters E_c, β_1 , S_r and S_c Theseresults are in agreement with the results those obtained by Hayat et al. [23].

Finally, the trapping phenomenon is taken into account. The numerical calculations give the following results:

(1) In case of the absence of E_c, the influence of $D_a$is the same as the influence of G_{rT} on the bolus size.

(2) In case of the presence of E_c, the influence of $D_a$on the size of the trapped bolus is contrary to the influence of G_{rT}. These results are in agreement with the results those obtained by Noreen [25] and Akbar et al. [26].

(3) Contour plots for radial and axial velocities respectively are illustrated through Figs. 6a and 6b.

Nomenclature

a	initial radius of the tube	T_0	stagnation temperature
b	amplitude of the peristaltic wave	T_m	mean fluid temperature
B_0	magnetic field strength	t	time
C	concentration of the fluid	U	radial velocity of the fixed frame
C_0	stagnation concentration	u	dimensionless radial velocity
c_p	specific heat parameter	V	velocity vector
C	wave propagation speed	W	axial velocity of the fixed frame
D	coefficient of mass diffusivity	w	dimensionless axial velocity
Da	Darcy number	Z	axial coordinate
E_c	Eckert number	z	dimensionless axial coordinate
e	electric charge		***Greek symbols***
G_{rC}	modified Grashof number	α_C	coefficient of mass expansion
G_{rT}	thermal Grashof number	α_T	coefficient of thermal expansion
g	gravitational acceleration	β	dimensionless Casson parameter
K	thermal conductivity	β_1	dimensionless heat source parameter
K_0	permeability of porous medium	γ	chemical reaction parameter
K_1	constant of chemical reaction	δ	wave number
K_T	thermal diffusion ratio	θ	heat capacity of the fluid
k^*	mean absorption coefficient	λ	wave length
M	Hartmann number	μ	fluid viscosity
m	Hall parameter	μ_B	plastic dynamic viscosity
n_e	number of electrons	ν	kinematic viscosity
P	fluid pressure	π	deformation rate product ($e_{ij}e_{ij}$)
P_r	Prandtl number	π_c	critical value of deformation rate
p_y	yield stress	ρ	fluid density
Q_0	constant of heat generation	σ	electric conductivity
R	along the radial coordinate	σ^*	Stefan Boltzmann constant
R_e	Reynolds number	τ_{ij}	stress tensor for Casson model
R_n	radiation parameter	Φ	dimensionless concentration
r	dimensionless radial coordinate	$\emptyset$	amplitude ratio
S_c	Schmidt number	ψ	stream function
S_r	Soret number		

References

[1] Hina, S., *et al.*, Influence of Compliant Walls on Peristaltic Motion with Heat/Mass Transfer and Chemical Reaction, *International Journal of Heat and Mass Transfer, 55* (2012), pp. 3386-3394.

[2] Noreen, S., Qasim, M., Peristaltic Flow with Inclined Magnetic Field and Convective Boundary Conditions, *Applied Bionics and Biomechanics, 11* (2014), pp.61-67.

[3] El-Dabe, N. T., *et al.*, Magneto Hydrodynamic Peristaltic Flow of Jeffery Nanofluid with Heat Transfer through a Porous Medium in a Vertical Tube, *Applied Mathematics and Information Sciences, 11* (2017), 4, pp.1097-1103.

[4] Shaaban, A. A., Abou-zeid, M. Y., Effects of Heat and Mass Transfer on MHD Peristaltic Flow of a Non-Newtonian Fluid through a Porous Medium between Two Coaxial Cylinders, *Mathematical Problems in Engineering, 2013* (2013), pp.1-11.

[5] Hayat, T., *et al.*, Peristaltic Flow of Sutterby Fluid Channel with Radiative Heat Transfer and Compliant Walls: A numerical study, *Results in Physics, 6* (2016), pp. 805-810.

[6] Nadeem, S., Akram, S., Heat Transfer in a Peristaltic Flow of MHD Fluid with Partial Slip, *Commun Nonlinear Sci Numer Simulat, 15* (2010), pp. 312-321.

[7] Hayat, T., *et al.*, Effects of Hall Current on Unsteady Flow of a Second Grade Fluid in a Rotating System, *Chemical Engineering Communications, 192* (2005), pp. 1272-1284.

[8] Mehmood, O.U., *et al.*, Non-Linear Peristaltic Flow of Walter's B Fluid in an Asymmetric Channel with Heat Transfer and Chemical Reactions, *Thermal Sci., 18*(2014), 4, pp.1065-1107.

[9] Eldabe, N. T., *et al.*, Hall Effects on the Peristaltic Transport of Williamson Fluid through a Porous Medium with Heat and Mass Transfer, *Applied Mathematical Modelling, 40* (2016), pp. 315-328.

[10] El Koumy, S. R., *et al.*, Hall and Porous Boundaries Effects on Peristaltic Transport Through Porous Medium of a Maxwell Model, *Transport Porous Medium, 94* (2012), pp.643-658.

[11] Akbar, N. S., *et al.*, MHD Dissipative Flow and Heat Transfer of Casson Fluids due to Metachronal Wave Propulsion of Beating Cilia with Thermal and Velocity Slip Effects Under an Oblique Magnetic Field, *Acta Astronautica, 128* (2016), pp. 1-12.

[12] Arthur, E. M., *et al.*, Analysis of Casson Fluid Flow Over a Vertical Porous Surface with Chemical Reaction in the Presence of Magnetic Field, *Journal of Applied Mathematics and Physics, 3*(2015), pp. 713-723.

[13] Ali, K., *et al.*, On Combined Effect of Thermal Radiation and Viscous Dissipation in Hydromagnetic Micropolar Fluid Flow Between two Stretchable Disks, *Thermal Sci.*,21(2017), 5, pp. 2155-2166.

[14] Elbashbeshy, E. M. A., *et al.*, Effects of Pressure Stress Work and Thermal Radiation on Free Convection Flow around a Sphere Embedded in a Porous Medium with Newtonian Heating, *Thermal Sci.*, 22 (2018), 1B, pp. 401-412.

[15] Eldabe, N., Abou-zeid, M., Radially Varying Magnetic Field Effect on Peristaltic Motion with Heat and Mass Transfer of a Non-Newtonian Fluid between Two Co-Axial Tubes, *Thermal Sci.*, 2016, pp. 1-13, DOI No. (10.2298).

[16] Vasudev, C., *et al.*, Peristaltic Flow of a Newtonian Fluid through a Porous Medium in a Vertical Tube under the Effect of a Magnetic Field. *International Journal of Current Scientific Research, 1* (2011), 3, pp. 105-110.

[17] He, J. H., Homotopy Perturbation Technique, *Computer Methods in Applied Mechanics and Engineering, 178* (1999), 3, pp. 257-262.
[18] Kumar. H., Homotopy Perturbation Method Analysis to MHD Flow of a Radiative NanoFluid with Viscous Dissipation and Ohmic Heating over a Stretching Porous Plate, Thermal *Sci.*, *22(*2018), 1B, pp. 413–422.
[19] Rajeev, Homotopy Perturbation Method for a Stefan Problem with Variable Latent Heat, *Thermal Sci.*, *18* (2014), pp. 391–398.
[20] Abou-zeid, M.,Homotopy Perturbation Method to MHD Non-Newtonian NanoFluid Flow through a Porous Medium in Eccentric Annuli with Peristalsis, *Thermal Sci.,21*(2017), 5, pp. 2069-2080.
[21] Abou-zeid, M., Effects of Thermal-Diffusion and Viscous Dissipation on Peristaltic Flow of Micropolar Non-Newtonian Nanofluid: Application of Homotopy Perturbation Method, *Results in Physics*, *6* (2016), pp. 481-495.
[22] Abou-zeid, M. Y., *et al.*, Numerical Treatment and Global Error Estimation of Natural Convective Effects on Gliding Motion of Bacteria on a Power-Law Nanoslime Through a Non-Darcy Porous Medium, *Journal of Porous Media, 18* (2015), 11, pp. 1091-1106
[23] Hayat, T., *et al.*, Heat and Mass Transfer Effects on Peristaltic Flow of an Oldroyd-B Fluid in a Channel with Compliant Walls, *Heat Transfer-Asian Research, 41* (2012), 1, pp. 63-83.
[24] Ali, N., *et al.*, Slip Effects on the Peristaltic Flow of a Third Grade Fluid in a Circular Cylindrical Tube, *Journal of Applied Mechanics, 76* (2009), pp. 1-10
[25] Noreen, S., Mixed Convection Peristaltic Flow of Third Order Nanofluid with an Induced Magnetic Field, *PLOS ONE, 8* (2013), 11, pp. 1-15.
[26] Akbar, N. S., *et al.*, Nano Fluid Flow in Tapering Stenosed Arteries with Permeable Walls, *International Journal of Thermal Sci., 85* (2014),pp. 54-61.